

SUPPORTING MATERIAL

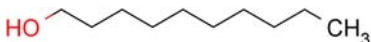
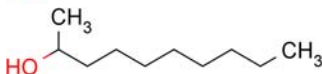
Alcohol effects on lipid bilayer properties

Authors: Helgi I. Ingólfsson and Olaf S. Andersen

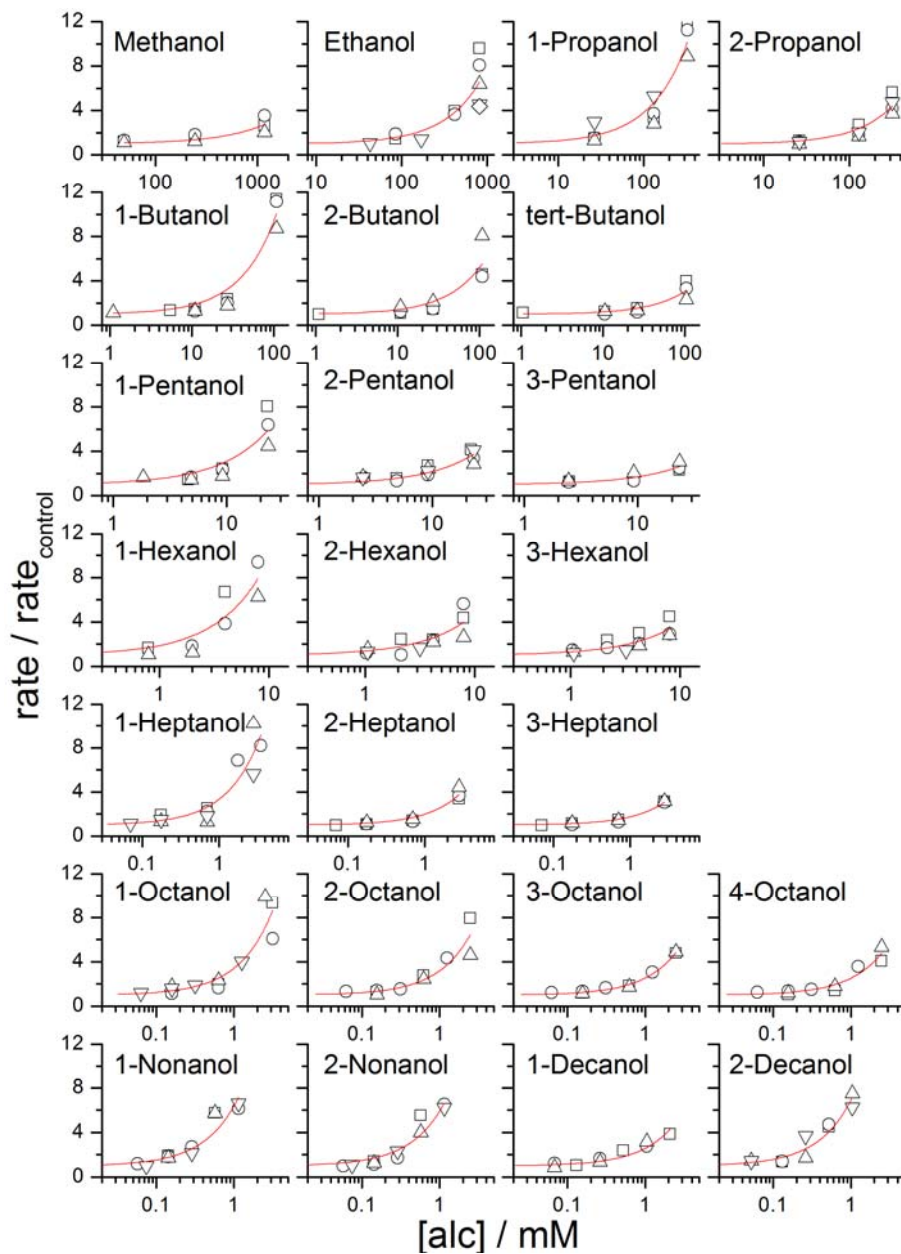
SUPPLEMENTAL TABLE S1

Alcohol properties

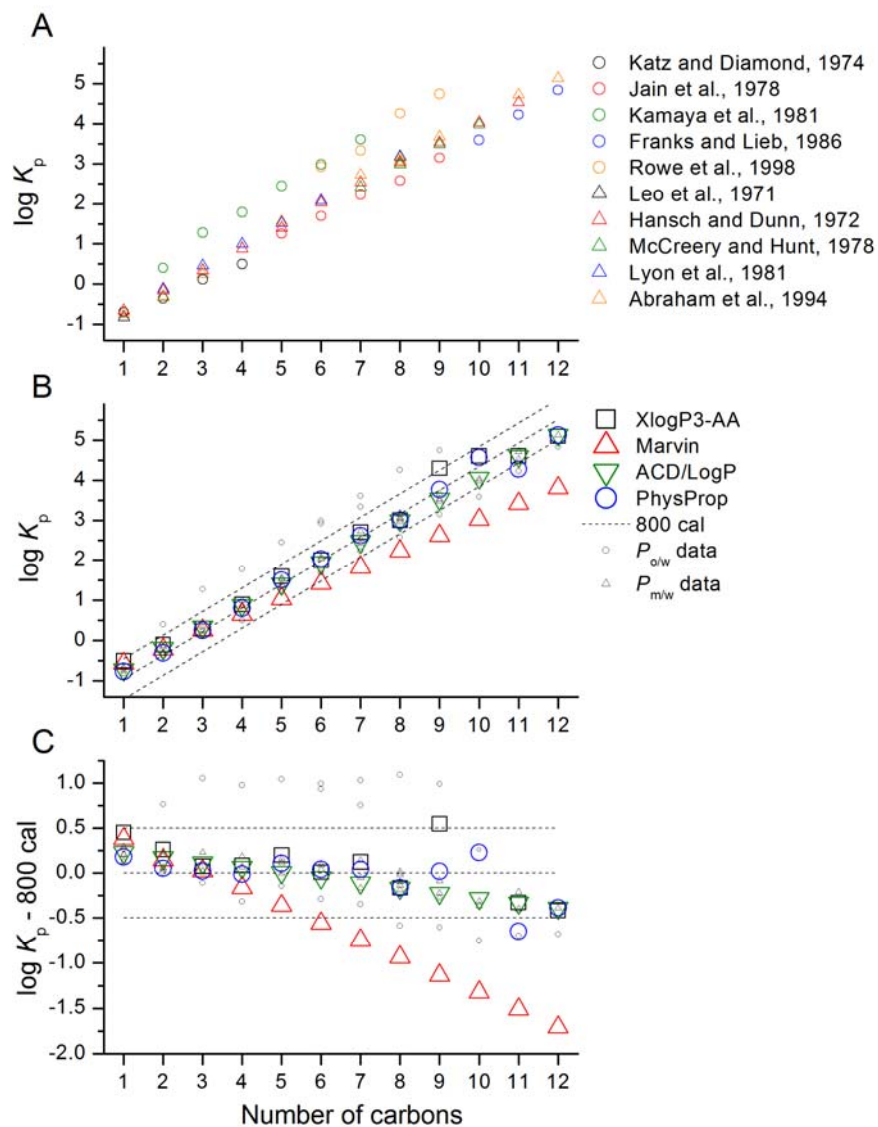
Name*	Structure [†]	MW [‡]	D^{\ddagger} (mM)	cLogP [§]	m_{alc}
Methanol		32.0	665.9±77.6	-0.72	0.10
Ethanol		46.1	146.7±13.3	-0.19	0.08
1-Propanol		60.1	35.52±2.07	0.34	0.07
2-Propanol		60.1	93.29±5.95	0.16	0.11
1-Butanol		74.1	11.94±0.66	0.88	0.08
2-Butanol		74.1	23.69±2.63	0.69	0.10
tert-Butanol		74.1	48.27±4.54	0.51	0.12
1-Pentanol		88.2	4.73±0.46	1.41	0.10
2-Pentanol		88.1	8.44±0.55	1.22	0.11
3-Pentanol		88.1	14.23±1.14	1.22	0.18
1-Hexanol		102.2	1.15±0.12	1.94	0.08
2-Hexanol		102.2	2.68±0.29	1.75	0.12
3-Hexanol		102.2	3.36±0.32	1.75	0.15
1-Heptanol		116.2	0.43±0.04	2.47	0.10
2-Heptanol		116.2	1.02±0.06	2.29	0.15
3-Heptanol		116.2	1.36±0.03	2.29	0.19
1-Octanol		130.2	0.41±0.03	3.00	0.24
2-Octanol		130.2	0.46±0.04	2.82	0.20
3-Octanol		130.2	0.65±0.01	2.82	0.26
4-Octanol		130.2	0.66±0.04	2.82	0.26
1-Nonanol		144.3	0.19±0.01	3.53	0.26
2-Nonanol		144.3	0.20±0.01	3.35	0.23

1-Decanol		158.3	0.63±0.04	4.06	0.68
2-Decanol		158.3	0.17±0.01	3.88	0.33

Name**, alcohol name. †**Structures** were drawn using MarvinSketch 5.0.3 from ChemAxon (Budapest, Hungary). ‡**MW**, molecular weight (g/mole). †**D**, concentration (mM) at which the alcohol doubles the fluorescence quenching rate. §**cLogP**, calculated octanol/water partitioning values, obtained using the ACD/Labs logP (1) algorithm (see Supplemental Methods). ‖m_{alc}***, mole fraction of alcohol in the bilayer at *D*, see Supplemental Methods.

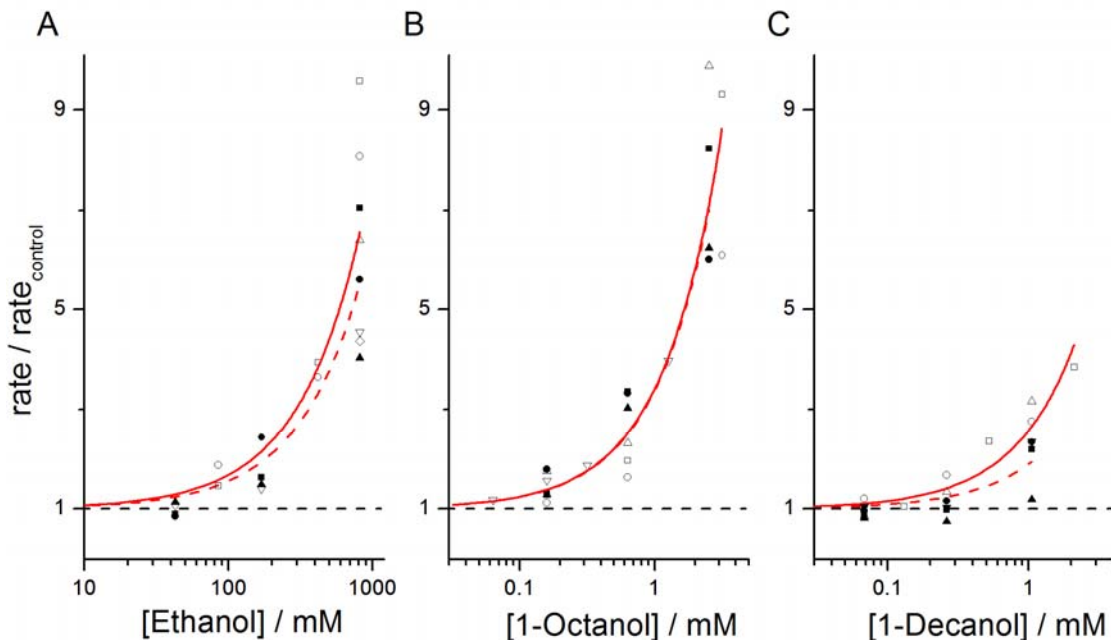


SUPPLEMENTAL FIGURE S1 The relative changes in fluorescence quenching rate as a function of alcohol concentration. Each alcohol was measured on at least three independent days of experiments (*differently shaped symbols*). For each alcohol, the fluorescence quenching rate was normalized to the rate in the absence of alcohol for that experiment. The control rates ranged from 15 to 50 with 29 ± 7 (mean \pm SD). The *red solid lines* are $f([\text{alc}]) = 1 + [\text{alc}]/D$ fits to the results. Notice the different x-axis scales for the different alcohol chain lengths.

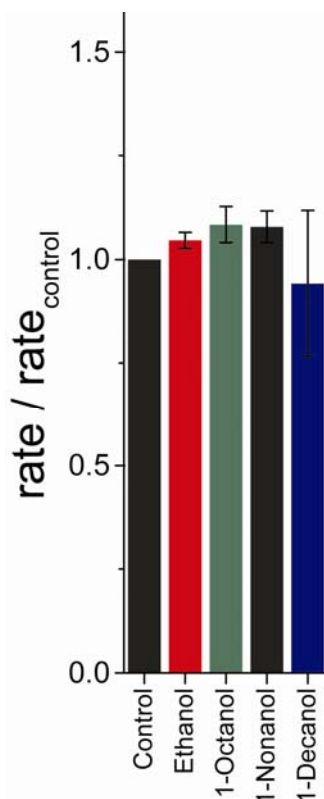


SUPPLEMENTAL FIGURE S2 Evaluating straight-chain alcohol/lipid partition coefficients.

(A) Experimental partition coefficients (K_p) for octanol/water (*triangles*) and various lipid bilayers/water (*circles*). (B) Octanol/water K_p , estimated using the XlogP3-AA algorithm (2), the logP plugin in MarvinSketch (3), and the ACD/Labs logP algorithm (1), as well as experimental values and estimates from the PhysProp database (SRC, Syracuse, NY). All experimental data from (A) are included as *small black symbols*; the *dashed lines* have slopes of 0.59, representing 800 cal/mole per $-\text{CH}_2$ group. (C) Same data as in (B), except that the middle 800 cal/mole line in B has been subtracted from all values to better visualize any data disparity.

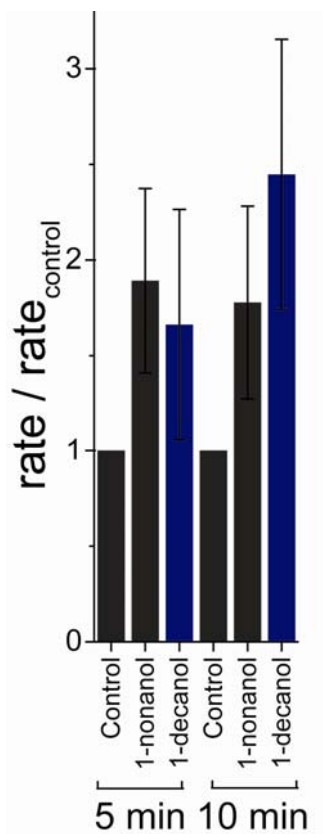


SUPPLEMENTAL FIGURE S3 Testing for aqueous phase depletion. The effect of doubling the assays lipid concentration. The relative changes in the rate of fluorescence quenching are shown for (A) ethanol, (B) 1-octanol and (C) 1-decanol. Results using the assay's standard lipid concentration are shown with *open symbols*, results using twice the lipid concentration are shown with *solid symbols*. Each alcohol was measured on at least three independent days of experiments (*differently shaped symbols*), the *red solid lines* (regular lipid concentration) and *red dotted lines* (double lipid concentration) are $f([\text{alc}]) = 1 + [\text{alc}]/D$ fits to the results. Only in (C) is the double lipid concentration (*red dotted line*) shifted significantly (p-value < 0.05) compared to the standard lipid concentration (*red solid line*).



SUPPLEMENTAL FIGURE S4 Alcohol bilayer-perturbing effects in a thinner bilayer.

Fluorophore-loaded LUVs were made using the shorter DC_{20:1}PC lipid and 26 nM of gA was added to the vesicles. Yet there are more conducting gA channels per vesicle than in the experiments in **Figs. 1-3** (see Supplemental Methods); thus, if present, any bilayer defects would be expected to have more pronounced effects in the thinner membranes. The alcohols, however, had much less effect than in **Figs. 1-3**, due to the reduced hydrophobic mismatch in the thinner bilayer, effectively excluding that the alcohols promoted the leakage of Tl⁺ along pathways at the channel/bilayer boundary. The effects of ethanol (*red*), 1-octanol (*green*), 1-nonanol (*black*), and 1-decanol (*blue*) were determined at twice their doubling rate concentration (*D*) in the thicker DC_{22:1}PC membranes (294, 0.82, 0.38, and 1.26 mM respectively). Average and SD of the relative change in quenching rates following the alcohol addition.



SUPPLEMENTAL FIGURE S5 Effect of varying the alcohol incubation time. The effects of 1-nonanol (*black*) and 1-decanol (*blue*) were determined at D (0.19 and 0.63 mM respectively) and incubated at 25°C for 5 or 10 min. Average and SD of the relative change in quenching rates as a function of added alcohols.

Supplemental Methods

The gA-based fluorescence assay was performed as described in (4, 5), which probes how the partitioning of amphiphiles, such as alcohols, into lipid bilayers alters the gA monomer \leftrightarrow dimer equilibrium, which is sensitive to changes in lipid bilayer thickness and changes in lipid bilayer physical properties (6).

Large unilamellar vesicles (LUVs) were prepared with the encapsulated fluorophore, 8-aminonaphthalene-1,3,6-trisulfonic acid (ANTS) using a combination of hydration, sonication, freeze-thawing and mini-extrusion. The vesicle-forming lipid was 1,2-dierucoyl-*sn*-glycero-3-phosphocholine (DC_{22:1}PC), this lipid was selected because it forms bilayers with a low permeability to the quencher (TI⁺) and with the gA monomer \leftrightarrow dimer equilibrium shifted toward the non-conducting monomers—but still poised such that we can observe changes in either direction (4). In the thinner 1,2-dioleoyl-*sn*-glycero-3-phosphocholine (DC_{18:1}PC) and 1,2-dieicosenoyl-*sn*-glycero-3-phosphocholine (DC_{20:1}PC) bilayers, the TI⁺ permeability is much higher than in the DC_{22:1}PC bilayers—and the gA monomer \leftrightarrow dimer equilibrium shifted strongly toward the conducting dimers, making it difficult to detect changes in the dimerization. The experiments in the DC_{20:1}PC LUVs therefore were done with 10-fold lower gA concentration, compared to the DC_{22:1}PC LUVs. But we still observed absolute quencher influx rates that were more than two-fold larger than those observed in the standard (DC_{22:1}PC) LUVs (data not shown), and the alcohols cause only small shifts in the monomer \leftrightarrow dimer equilibrium (as evident from the minimal changes in the quencher influx rate, **Fig. S4**).

DC_{22:1}PC has a gel-liquid crystal phase transition temperature around 11 °C (7). Alcohols can both decrease and, in the case of the long-chain alcohols, also increase the phase transition temperature, but at the mole-fractions used here the changes are modest—the alcohol-induced shift in the phase transition temperature in (usually saturated) phosphatidylcholine bilayers are reported to be less than 5 °C at mole-fractions of 0.2 (8-11). If the ANTS-containing vesicles are cooled to below their phase transition temperature, the fluorescent dye leaks out. When we store the vesicles at 12.5 °C in the presence of the long-chain alcohols for 24 h there is

no dye leakage; similarly, when we incubate the LUVs with any of the alcohols at 25 °C, there was no dye leakage with any of the alcohols—even at the highest concentration tested. The changes in quenching rate therefore are not caused by alcohol-induced changes in the gel-liquid crystal phase transition temperature.

The DC_{22:1}PC (in chloroform) was dried under nitrogen and further dried in a desiccator under vacuum overnight to fully remove the chloroform. The lipid was rehydrated in 100 mM NaNO₃, 25 mM ANTS and 10 mM HEPES at pH 7.0 at room temperature overnight. The lipid suspension was then sonicated in a low power sonicator for 1-2 min, freeze-thawed 5-6 times, and extruded 21 times through a 0.1 μm polycarbonate membrane filter. Extravesicular ANTS was removed using a PD-10 Desalting column (GE Healthcare, Piscataway, NJ), and the solution was stored at 12 °C in the dark for a maximum of ten days. 24 hours before each experiment, the ANTS-loaded LUV suspension was further diluted to a final lipid concentration of ~200 μM in 140 mM NaNO₃, 10 mM HEPES, pH 7.0 (25 mM internal ANTS), and a portion of the vesicles were incubated with 260 nM gA from *Bacillus brevis* (Sigma Chemical Co). gA and the alcohols tested at low concentrations (chain lengths ≤ 7) were diluted in dimethyl sulfoxide (DMSO) (Burdick & Jackson, Muskegon, MI). A few alcohols (chain lengths between 6 and 8), used at intermediate concentrations, were tested dissolved in DMSO and without DMSO, with no discernible difference. The total solvent (DMSO) concentration was kept constant between the tested samples and controls, never exceeding 0.6%, a concentration that has little effect on the quenching rate (4). The alcohols were incubated for 10 min at 25°C with the final ANTS-loaded LUV suspension. The 10 min incubation time was sufficient to equilibrate the alcohols, as 1-nonanol and 1-decanol incubated for 5 or 10 min showed no apparent difference in activity, **Fig. S5**.

The fluorescence time courses were recorded for a 1:1 mixture of ANTS-loaded LUV sample and buffer (140 mM NaNO₃, 10 mM HEPES, pH 7.0) or quencher (50 mM TINO₃, 94 mM NaNO₃, 10 mM HEPES, pH 7.0) solution rapidly mixed using a SX.20 Stopped-Flow Spectrometer with a 150-W xenon lamp and a sampling rate set to 5,000 points/s. Excitation was

set at 352 nm and the fluorescence emission was recorded above 455 nm, using a high-pass filter. The traces were analyzed using MATLAB 7.4 (The MathWorks, Inc, Natick, MA). For each sample the fluorescence was normalized to the average of the first 2-10 ms buffer values and a stretched exponential (12) was fit to the first 2–100 ms for each quencher run. Due to the stochastic nature of gA channel distribution between the vesicles and the un-uniformity in the LUVs size distribution the quenching time courses follow a multi-exponential distribution. This multi-exponential time course was fitted by a stretched exponential:

$$F(t) = F(\infty) + (F(0) - F(\infty)) \cdot \exp\left\{-\left(t / \tau_0\right)^\beta\right\},$$

where $F(t)$ is the fluorescence at time t and β ranges between 0 and 1 and depends on the degree of multi-exponentiality of the distribution. The fluorescence quenching rates is then calculated as:

$$k(t) = (\beta / \tau_0) \cdot (t / \tau_0)^{(\beta-1)}$$

For additional details on the influx rate quantification see appending in (4). Each sample was measured at least seven times and a average of the quenching rates at 2 ms was calculated. Each alcohol was tested on at least three different occasions/days of experiments.

Alcohol Membrane Partition Coefficients

Determining reasonable/consistent estimates for the membrane/aqueous partition coefficients ($P_{m/w}$) for all the alcohols tested turned out to be more difficult than expected. A compound's partition coefficient (K_p) indicates the compound's relative preference for one medium over the other and will vary depending on the composition of the two media, pH, temperature and the mole fraction of the compound in the two phases (13-17). Alcohols' do not have titratable groups, and their K_p s should not be pH dependent. Alcohol bilayer/aqueous K_p s have been determined by many investigators, using a variety of methods and systems. Katz and Diamond (18, 19) determined K_p s into dimyristoyl lecithin liposomes over a range of temperatures using ^{14}C -labeled compounds; 25 °C results for four straight-chain alcohols are

shown in **Fig. S3 A** (black circles). Jain et al. (20) evaluated the bilayer-perturbing ability and K_{ps} of alkanols using a variety of methods; included in **Fig. S3 A** (red circles) are five straight-chain alcohol K_{ps} between aqueous phase and phosphatidylcholine liposomes, measured with gas chromatography. Kamaya et al. (21) measured K_{ps} for six straight-chain alcohols into phosphatidylcholine liposomes, using the shift in the liposome phase-transition temperature, green circles in **Fig. S3 A**. Franks and Lieb (22) determined the membrane/buffer partitioning of a few long-chain alcohols, including three shown in **Fig. S3 A** (blue circles), using alcohol quenching of the firefly luciferase. Rowe and colleagues (23) determined the partitioning of four straight-chain alcohols into lipid vesicles composed of various lipid types using titration calorimetry. **Fig. S3 A** (orange circles) shows results for dipalmitoylphosphatidylcholine (DPPC) lipid vesicles at 45°C.

There is considerable variability among the measured alcohol $P_{m/w}$ s obtained using different methods (**Fig. S3 A**, circles). This may reflect, in part, differences in experimental approaches and/or systems used. For example, in isothermal titration calorimetric (ITC) studies on 1-butanol partitioning into DPPC lipid vesicles, $P_{m/w}$ varied more than 2.5-fold over a 40°C change in temperature, with discreet jumps corresponding to the changes in the lipid phase (24). Experiments using headspace gas chromatography (25) and ITC (23) as well as statistical thermodynamics predictions (26), suggest that $P_{m/w}$ for short-chain alcohols may vary two-fold depending on the bilayer lipids' acyl chain length and saturation, lipid head group and cholesterol content. Yet, despite the variability between the results obtained using these different methods, the decrease in the free energy of partitioning with each successively longer alcohol (determined using the same method) tends to be constant, see **Fig. S3 A**; being 700-800 cal/mole for each added -CH₂ group (21, 22, 27-29).

Octanol/water partition coefficients ($P_{o/w}$) are often used as proxies for molecules' bilayer/aqueous phase partition coefficients, especially for neutral solutes; they are easier to measure and provide a standard reference phase for comparison between compounds (16, 17). $P_{o/w}$ measurements are more consistent than general membrane/aqueous phase measurements

(**Fig. S3 A** triangles vs. circles). Leo and colleagues (30), in their classic review on partition coefficients between polar and nonpolar phases, describe equations for converting between $K_{p,s}$ into different phases, and report an extensive list of experimentally determined partition coefficients. **Fig. S3 A** includes seven straight-chain alcohols $P_{o/w,s}$ from that list (black triangles). Hansch and Dunn (31) reported experimentally determined $P_{o/w,s}$ as well as estimates calculated from additivity principles (32), **Fig. S3 A** (red triangles). McCreery and Hunt (33) report membrane/buffer $K_{p,s}$ for dozens of alcohols, including ten straight-chain alcohols. The membrane/buffer partition coefficients were derived from $P_{o/w,s}$ by dividing by 5 (the $P_{o/w,s}$ were experimentally determined or estimates)—these values were converted back to $P_{o/w}$ and are shown in **Fig. S3 A** (green triangles). Lyon et al. (34) report membrane partition coefficients for a number of alcohols, including six straight-chain alcohols. For the shorter alcohols they use oil/water partition data from (35), convert them to $P_{o/w,s}$ using the solvent regression equation, determined by (30), and divide by 5 to get membrane/water partitioning. For the longer alcohols, they linearly extrapolated from the measured $\log P_{o/w}$ values. The straight-chain alcohol values were converted back to $P_{o/w}$ and included in **Fig. S3 A** (blue triangles). Abraham and colleagues (36, 37) analyzed and predicted physiochemical properties for a large set of molecules, including eleven straight-chain alcohols in **Fig. S3 A** (orange triangles). The compounds $P_{o/w}$ values are derived from multiple sources, including gaseous solubility experiments.

In addition to $P_{o/w}$ values being more consistent than $P_{m/w}$ values, numerous methods have been developed to calculate $P_{o/w}$ values; for reviews on calculated octanol/water partition coefficients (cLogP) methods see (38, 39). **Fig. S3 B** shows the experimental data from **Fig. S3 A** (small black symbols) overlaid with cLogP from: the XlogP3-AA (2) algorithm, logP plugin in MarvinSketch (3) ChemAxon Ltd. (Budapest, Hungary), and the ACD/Labs logP (1) Advanced Chemistry Development, Inc. (Toronto, Canada) algorithm. **Fig. S3 B** shows both experimental and estimated values from the PhysProp database SRC (Syracuse, NY). The three evenly spaced dashed black lines have a slope of 0.59, representing about 800 cal/mole decrease in the free energy of partitioning for each $-\text{CH}_2$ group in the straight-chain alcohols. **Fig. S3 C** shows the

same data as **Fig. S3 B** but with the middle 800 cal line being subtracted from all the results to better illustrate the difference between the K_p s and the different cLogP methods. From the comparison in **Fig. S3 C** we chose the cLogP values from the ACD/Labs logP (1) algorithm as estimates for the membrane/aqueous phase partitioning for all the alcohols in this study; see **Table S1** for the cLogP values.

Alcohol to Lipid Mole Fraction

The alcohols' membrane concentrations ($[\text{alc}]_m$) were estimated as in (4, 40, 41). The calculated octanol/water partition coefficients (cLogP) using the ACD/Labs logP algorithm (1) from Advanced Chemistry Development, Inc. (where located) were used as a substitute for alcohol lipid bilayer/aqueous phase partition coefficients (K_p s); see above for discussion/evaluation of the selected partitioning values. The membrane alcohol concentration ($[\text{alc}]_m$) is:

$$[\text{alc}]_m = K_p \times [\text{alc}]_a, \quad (1)$$

where $[\text{alc}]_a$ is the alcohol concentration in the aqueous phase. **Eq. 1** is valid in the limit of infinite water to lipid volume ratio ($r_{a/m}$). With finite water to lipid volume ratio, the alcohol partitioning into the bilayer decreases $[\text{alc}]_a$ below the nominal concentration—where the nominal concentration ($[\text{alc}]_{\text{nom}}$) is the concentration added, with no depletion due to bilayer partitioning. The alcohol bilayer ($[\text{alc}]_m$) and aqueous ($[\text{alc}]_a$) phase concentrations are related as:

$$[\text{alc}]_a = \frac{r_{a/m}}{K_p + r_{a/m}} [\text{alc}]_{\text{nom}}, \quad (2)$$

$$[\text{alc}]_m = \frac{K_p \times r_{a/m}}{K_p + r_{a/m}} [\text{alc}]_{\text{nom}}. \quad (3)$$

From **Eq. 3** we get the alcohol to lipid mole fraction in the membrane phase (m_{alc}):

$$m_{\text{AM}} = \frac{[\text{alc}]_m}{[\text{alc}]_m + [\text{L}]_m}, \quad (4)$$

where $[L]_m$ is the molar lipid concentration in the membrane phase. In our case $[L]_m \approx 1.1$ M and $r_{a/m} \approx 5500$.

Supplemental References

1. Petrauskas, A., and E. Kolovanov. 2000. ACD/Log P method description. *Persp. in Drug Discovery and Design* 19:99-116.
2. Cheng, T., Y. Zhao, X. Li, F. Lin, Y. Xu, X. Zhang, Y. Li, R. Wang, and L. Lai. 2007. Computation of octanol-water partition coefficients by guiding an additive model with knowledge. *J. Chem. Inf. Model.* 47:2140-2148.
3. Viswanadhan, V. N., A. K. Ghose, G. R. Revankar, and R. K. Robins. 1989. Atomic physicochemical parameters for three dimensional structure directed quantitative structure-activity relationships. 4. Additional parameters for hydrophobic and dispersive interactions and their application for an automated superposition of certain naturally occurring nucleoside antibiotics. *J. Chem. Inf. Comput. Sci.* 29:163-172.
4. Ingólfsson, H. I., and O. S. Andersen. 2010. Screening for small molecules' bilayer-modifying potential using a gramicidin-based fluorescence assay. *Assay Drug Dev. Technol.* 8:427-436.
5. Ingólfsson, H. I., R. L. Sanford, R. Kapoor, and O. S. Andersen. 2010. Gramicidin-based fluorescence assay; for determining small molecules potential for modifying lipid bilayer properties. *J. Vis. Exp.*
6. Lundbæk, J. A., S. A. Collingwood, H. I. Ingólfsson, R. Kapoor, and O. S. Andersen. 2010. Lipid bilayer regulation of membrane protein function: gramicidin channels as molecular force probes. *J. R. Soc. Interface* 7:373-395.
7. Caffrey, M., and G. W. Feigenson. 1981. Fluorescence quenching in model membranes. 3. Relationship between calcium adenosinetriphosphatase enzyme activity and the affinity of the protein for phosphatidylcholines with different acyl chain characteristics. *Biochemistry* 20:1949-1961.
8. Lee, A. G. 1976. Interactions between anesthetics and lipid mixtures. Normal alcohols. *Biochemistry* 15:2448-2454.
9. Rowe, E. S. 1985. Thermodynamic reversibility of phase transitions. Specific effects of alcohols on phosphatidylcholines. *Biochim Biophys Acta* 813:321-330.
10. Kamaya, H., S. M. Ma, and S. H. Lin. 1986. Dose-dependent nonlinear response of the main phase-transition temperature of phospholipid membranes to alcohols. *J. Membr. Biol.* 90:157-161.
11. Li, S., H. N. Lin, G. Wang, and C. Huang. 1996. Effects of alcohols on the phase transition temperatures of mixed-chain phosphatidylcholines. *Biophys J* 70:2784-2794.
12. Berberan-Santos, M. N., E. N. Bodunov, and B. Valeur. 2005. Mathematical functions for the analysis of luminescence decays with underlying distributions 1. Kohlrausch decay function (stretched exponential). *Chem. Phys.* 315:171-182.

13. De Young, L. R., and K. A. Dill. 1988. Solute partitioning into lipid bilayer membranes. *Biochemistry* 27:5281-5289.
14. Peitzsch, R. M., and S. McLaughlin. 1993. Binding of acylated peptides and fatty acids to phospholipid vesicles: pertinence to myristoylated proteins. *Biochemistry* 32:10436-10443.
15. White, S. H., W. C. Wimley, A. S. Ladokhin, and K. Hristova. 1998. Protein folding in membranes: determining energetics of peptide-bilayer interactions. *Meth. Enzymol.* 295:62-87.
16. Avdeef, A. 2001. Physicochemical profiling (solubility, permeability and charge state). *Curr. Top. Med. Chem.* 1:277-351.
17. Seydel, J. K., and M. Wiese. 2002. Drug-Membrane Interactions: Analysis, Drug Distribution, Modeling. Wiley-VCH, Weinheim.
18. Katz, Y., and J. M. Diamond. 1974. A method for measuring nonelectrolyte partition coefficients between liposomes and water. *J. Membr. Biol.* 17:69-86.
19. Katz, Y., and J. M. Diamond. 1974. Thermodynamic constants for nonelectrolyte partition between dimyristoyl lecithin and water. *J. Membr. Biol.* 17:101-120.
20. Jain, M. K., J. Gleeson, A. Upreti, and G. C. Upreti. 1978. Intrinsic perturbing ability of alkanols in lipid bilayers. *Biochim. Biophys. Acta.* 509:1-8.
21. Kamaya, H., S. Kaneshina, and I. Ueda. 1981. Partition equilibrium of inhalation anesthetics and alcohols between water and membranes of phospholipids with varying acyl chain-lengths. *Biochim. Biophys. Acta* 646:135-142.
22. Franks, N. P., and W. R. Lieb. 1986. Partitioning of long-chain alcohols into lipid bilayers: implications for mechanisms of general anesthesia. *Proc. Natl. Acad. Sci. USA* 83:5116-5120.
23. Rowe, E. S., F. Zhang, T. W. Leung, J. S. Parr, and P. T. Guy. 1998. Thermodynamics of membrane partitioning for a series of n-alcohols determined by titration calorimetry: role of hydrophobic effects. *Biochemistry* 37:2430-2440.
24. Zhang, F., and E. S. Rowe. 1992. Titration calorimetric and differential scanning calorimetric studies of the interactions of n-butanol with several phases of dipalmitoylphosphatidylcholine. *Biochemistry* 31:2005-2011.
25. Nizza, D. T., and K. Gawrisch. 2009. A layer model of ethanol partitioning into lipid membranes. *Gen. Physiol. Biophys.* 28:140-145.
26. Cantor, R. S. 2001. Bilayer Partition Coefficients of Alkanols: Predicted Effects of Varying Lipid Composition. *J. Phys. Chem. B* 105:7550-7553.
27. Schneider, H. 1968. The intramembrane location of alcohol anesthetics. *Biochim. Biophys. Acta - Biomembranes* 163:451-458.
28. Smith, R., and C. Tanford. 1973. Hydrophobicity of Long Chain n-Alkyl Carboxylic Acids, as Measured by Their Distribution Between Heptane and Aqueous Solutions. *Proc. Natl. Acad. Sci. USA* 70:289-293.

29. Jain, M. K., and N. M. Wu. 1977. Effect of small molecules on the dipalmitoyl lecithin liposomal bilayer: III. Phase transition in lipid bilayer. *J. Membr. Biol.* 34:157-201.
30. Leo, A., C. Hansch, and D. Elkins. 1971. Partition coefficients and their uses. *Chem. Rev.* 71:525-616.
31. Hansch, C., and W. J. Dunn, 3rd. 1972. Linear relationships between lipophilic character and biological activity of drugs. *J. Pharm. Sci.* 61:1-19.
32. Fujita, T., J. Iwasa, and C. Hansch. 1964. A New Substituent Constant, π , Derived from Partition Coefficients. *J. Am. Chem. Soc.* 86:5175-5180.
33. McCreery, M. J., and W. A. Hunt. 1978. Physico-chemical correlates of alcohol intoxication. *Neuropharmacology* 17:451-461.
34. Lyon, R. C., J. A. McComb, J. Schreurs, and D. B. Goldstein. 1981. A relationship between alcohol intoxication and the disordering of brain membranes by a series of short-chain alcohols. *J. Pharmacol. Exp. Ther.* 218:669-675.
35. Lindenberg, B. A. 1951. Lindenberg B.A. Sur La solubilités des substances organiques amphipatiques dans les glycerides neutres et hydroxyles. *J. Chim. Phys.* 48:350-355.
36. Abraham, M. H. 1993. Scales of solute hydrogen-bonding: their construction and application to physicochemical and biochemical processes. *Chem. Soc. Rev.* 22:73-83.
37. Abraham, M. H., H. S. Chadha, G. S. Whiting, and R. C. Mitchell. 1994. Hydrogen bonding. 32. An analysis of water-octanol and water-alkane partitioning and the $\Delta \log P$ parameter of Seiler. *J. Pharm. Sci.* 83:1085-1100.
38. Leo, A. J. 1993. Calculating $\log P_{oct}$ from structures. *Chem. Rev.* 93:1281-1306.
39. Eros, D., I. Kovesdi, L. Orfi, K. Takacs-Novak, G. Acsady, and G. Keri. 2002. Reliability of $\log P$ predictions based on calculated molecular descriptors: a critical review. *Curr. Med. Chem.* 9:1819-1829.
40. Bruno, M. J., R. E. I. Koeppe, and O. S. Andersen. 2007. Docosahexaenoic acid alters bilayer elastic properties. *Proc. Natl. Acad. Sci. USA* 104:9638-9643.
41. Ingólfsson, H. I., R. E. Koeppe II, and O. S. Andersen. 2007. Curcumin is a modulator of bilayer material properties. *Biochemistry* 46:10384-10391.